www.sciencemag.org/content/357/6356/1156/suppl/DC1

Supplementary Materials for

Potential role of intratumor bacteria in mediating tumor resistance to the chemotherapeutic drug gemcitabine

Leore T. Geller, Michal Barzily-Rokni, Tal Danino, Oliver H. Jonas, Noam Shental, Deborah Nejman, Nancy Gavert, Yaara Zwang, Zachary A. Cooper, Kevin Shee, Christoph A. Thaiss, Alexandre Reuben, Jonathan Livny, Roi Avraham, Dennie T. Frederick, Matteo Ligorio, Kelly Chatman, Stephen E. Johnston, Carrie M. Mosher, Alexander Brandis, Garold Fuks, Candice Gurbatri, Vancheswaran Gopalakrishnan, Michael Kim, Mark W. Hurd, Matthew Katz, Jason Fleming, Anirban Maitra, David A. Smith, Matt Skalak, Jeffrey Bu, Monia Michaud, Sunia A. Trauger, Iris Barshack, Talia Golan, Judith Sandbank, Keith T. Flaherty, Anna Mandinova, Wendy S. Garrett, Sarah P. Thayer, Cristina R. Ferrone, Curtis Huttenhower, Sangeeta N. Bhatia, Dirk Gevers, Jennifer A. Wargo, Todd R. Golub, Ravid Straussman*

*Corresponding author. Email: ravidst@weizmann.ac.il

Published 15 September 2017, *Science* **357**, 1156 (2017)
DOI: 10.1126/science.aah5043

This PDF file includes:

Other Supplementary Materials for this manuscript includes the following:
(available at www.sciencemag.org/content/357/6356/1156/suppl/DC1)

Tables S1 to S7 (Excel)

Materials and Methods

Cell lines and reagents

The sources of all cell lines and bacteria used are listed in table S1. All cells were maintained in Dulbecco's Modified Eagle's Medium (DMEM) (Invitrogen, #10569-010) containing 10% fetal bovine serum (FBS) and 1% penicillin-streptomycin and glutamine (Invitrogen, #15140-122). For expression of green fluorescent protein (GFP) in cancer cell lines, lentiviral transduction was carried out using the pLex_TRC206-GFP plasmid. Gemcitabine (G6423) and oxaliplatin (O9512) were purchased from Sigma.

Stroma-mediated chemoresistance co-culture screen

The full screen and method was previously described (*5*). In brief, on day 0, stromal cells (1,700 cells/well in 20 μl) were plated in 384-well clear-bottom plates (Corning, product #3712), together with GFP-labeled cancer cells (1,700 cells/well in 20 μl). On day 1, the cells were treated with 10μl 5X drug using the CyBi-Well Vario 384/25 Simultaneous Pipettor (CyBio). On day 4, the medium in all wells was replaced with fresh medium. GFP fluorescence was read on days 1, 4, and 7 using a SpectraMax M5e Microplate Reader (Molecular Devices). A fluorescence microscope with high-throughput screening capabilities (Axio Observer.Z1, Zeiss) was used to document bright-field and GFP images on day 7. All screens were carried out in quadruplicate.

Conditioned medium (CM) on cell culture screen

To prepare CM, stromal cells were cultured in 15 cm plates (Thermo Scientific, #168381). CM was harvested 3 days later, when plates were 80-90% confluent. CM was diluted 1:1 with fresh media. Experiments were performed according to the previously described co-culture experiment protocol, with the following changes: *i)* on day 0, 384-well plates were seeded with 20μl/well of CM instead of 20μl/well of stromal cells; *ii)* on day 1, the media from all wells were replaced with fresh CM; *iii)* on day 4, media were replaced with fresh CM instead of fresh media, before re-treating the cells with gemcitabine.

PCR for detection of *Mycoplasma*

The protocol is based on the Takara Kit (#6601). The buffer used, deoxynucleotide triphosphates (dNTPs) and Taq polymerase were obtained from the Takara Ex Taq kit (#RR001A). The following forward and reverse *Mycoplasma*-specific primers were used for PCR: 5'- ACACCATGGGAGCTGGTAAT-3',
5'- CTTCWATCGACTTYCAGACCCAAGGCAT-3'. PCR reactions contained 13.9 μl of Invitrogen UltraPure DDW (10977-015), 2 μl of buffer, 1.6 μl of dNTPs, 0.1 μl of TaKaRa Ex Taq ™, 0.5 μl of both forward and reverse primers (final concentration of 20 μM), and 2 μl of genomic DNA or 2 μl of CM. CM was collected after an incubation time of three days on cells, at which point the cells had reached at least 80% confluence. Reactions were held at 94°C for 30 s to denature the DNA, with amplification proceeding for 40 cycles at 94°C for 30 s, 55°C for 2 min, and 72°C for 1 min.

Eradication of *M. hyorhinis* from HDF cells by G418 Sulfate

HDF cells were infected with a lentivirus containing the pBabe-Neo plasmid to generate HDF cells with resistance to G418 Sulfate (Geneticin ®, Gibco #10131-027). Three days after the

lentiviral infection, cells were treated with 200 μg/ml of G418 for two weeks to eradicate the infection. After 1, 2, and 4 weeks of G418 treatment, cells were found to be negative for *Mycoplasma* infection by PCR.

M. hyorhinis positive or negative colon carcinoma mouse model

All animal work was approved by the Institutional Animal Care and Use Committee (Columbia, protocol AC-AAAN8002 and Massachusetts Institute of Technology (MIT), protocol 0414-022-17). The protocol requires animals to be euthanized when tumors reach 2 cm^3, or under veterinary staff recommendation. For all experiments, mice were blindly randomized into various groups using a random number generator. A subcutaneous model of colon carcinoma was generated by injecting 1×10^7 *M. hyorhinis* positive or negative luciferase expressing MC-26 mouse colon carcinoma cells subcutaneously into the flanks of immunocompetent, 6 week old, female BALB/c mice (Taconic Biosciences). MC-26 mouse colon carcinoma cells were grown in DMEM (10% FBS, 1% penicillin-streptomycin and glutamine) media. For subcutaneous tumor injection, animals were anesthetized using isoflurane. Gemcitabine was administered intraperitoneally (150mg/kg) on days 0, 4, and 9. Tumor size was monitored by reading of the firefly luciferase activity using the Spectrum in vivo imaging system (IVIS) (Caliper Life Sciences).

High-performance liquid chromatography-tandem mass spectrometry (HPLC-MS/MS) (The Broad Institute)

HPLC-MS/MS was performed on a Thermo Scientific LCMS system, which includes a TSQ Quantum Ultra triple-quad mass spectrometer, an Accela LC pump, and a Thermo Pal auto-sampler. Gemcitabine: ions monitored: 264.080/112.135 in positive ion mode, collision energy: 20v, tube lens offset voltage: 84v. dFdU: ions monitored: 263.048/220.074 in negative ion mode collision energy: 16v, tube lens offset voltage: 82v. LC method: solvent A: 5mM ammonium acetate, solvent B: 100% MeOH, column: Agilent Eclipse XDB-c18 2.1 x 50mm, flow rate: 100μl/min. This method was used for experiments described in Fig. 1C, figs. S4 and S5.

High-performance liquid chromatography-tandem mass spectrometry (HPLC-MS/MS) (The Weizmann Institute)

For determination of gemcitabine (dFdC) levels in samples, internal standard (IS) [$^{13}C_1$,$^{15}N_2$]-gemcitabine (Toronto Research Chemicals) diluted in double-distilled water (DDW) was added to each sample at a final concentration of 500 ng/ml.

The samples were then filtered through a 0.2-μm PTFE filter (Millex-LG, Millipore) into HPLC vials containing inserts.

The LC–MS/MS instrument consisted of an Acuity I-class UPLC system (Waters) and Xevo TQ-S triple quadruple mass spectrometer (Waters) equipped with an electrospray ion source and operated in positive ion mode was used for analysis of nucleoside monophosphates. MassLynx and TargetLynx software (version 4.1, Waters) were applied for the acquisition and analysis of data. Chromatographic separation was done on a 50 mm×2.1 mm internal diameter, 1.7-μm UPLC BEH C18 column equipped with 50 mm×2.1 mm internal diameter, 1.7-μm UPLC BEH C18 pre-column (both Waters Acuity) with mobile phases A (5 mM ammonium acetate, pH 6.8) and B (methanol) at a flow rate of 0.2 ml/min and column temperature 30°C. A gradient was used as follows,

%B (min.): 5 (0), 30 (1), 30 (3), 100 (3.5), 5 (4), 5 (5). Samples kept at 8°C were automatically injected in a volume of 1 µl. Retention time for gemcitabine and its labeled analog was 1.47 min.
For mass spectrometry, argon was used as the collision gas with a flow of 0.10 ml/min. The capillary voltage was set to 2.67 kV, cone voltage 25V, source temperature 150°C, desolvation temperature 400°C, and desolvation gas flow 800 L/hour. The analytes were detected using multiple-reaction monitoring: 264.1 > 95.0 m/z (collision energy CE=35eV) and 264.1 > 112.0 m/z (CE=10eV) for gemcitabine, and 267.0 > 97.0 m/z (CE=40eV) and 267.0 > 115.0 m/z (CE=15eV) for IS. This method was used for experiments described in Fig. 2B, figs. S7 and S9.

Bacteria-mediated gemcitabine resistance screen

Twenty-seven bacteria were cultured overnight in their respective growth conditions (table S1). The next morning, bacteria were diluted 1:25 in DMEM and transferred into 96-well U-shaped plates (BD Falcon #353077). Gemcitabine was then added to bacteria at a final concentration of 80X (40µM) and incubated with the bacteria for 3 hours at 37˚C. The bacteria-drug mix was then diluted 1:8 into 96-well filter plates (Pall #8119), and centrifuged at 1500 × g for 10 min at room temperature into 96-well receiver plates (VWR #82051-242). The final filtrate was added to GFP-labeled RKO human colorectal carcinoma cells (2,000 cells/well), resulting in a 1X concentration of 0.5µM gemcitabine. Cell growth was monitored for 7 days by reading GFP fluorescence.

Bacterial colonization of tumors

Six-week old, BALB/c female mice (Taconic Biosciences) were shaved and subcutaneously implanted with a luciferase (firefly) expressing MC-26 colon carcinoma cell line at a concentration of 1×10^7 cells/100 µl PBS per flank. For subcutaneous tumor cell injection, animals were anesthetized using isoflurane. Tumors were allowed to grow for approximately 2 weeks before they reached a size of 4-8 mm. Bacteria were grown overnight at 37˚C in their respective media (table S1). On the day of injection, bacteria were diluted 1:100 into fresh media and grown to OD600=0.4-0.6. Bacteria were then washed with PBS (0.22µm filtered) 3 times. Mice were injected with 5×10^6 bacteria in 100µl PBS through the tail vein.

Monitoring of tumor burden and bacterial populations

An *E. coli* Nissle 1917 strain was integrated with a chromosomal bacterial luciferase cassette (luxCDABE) (*23*). Luminescence signals were measured 48 hours post-injection (day 0 on x-axis), using the IVIS Spectrum imaging system (Caliper Life Sciences) set to the auto-exposure setting (typically 30-60 s). Living Image software (Caliper Life Sciences) was used for analysis.
To measure bacterial luciferase, a luminescence measurement was made before injection of luciferin, with an open filter. Mammalian luciferase (Firefly) measurements were made following bacterial luminescence measurement and 15 min post-intraperitoneal injection of 100µl of D-luciferin (30 mg/ml), with an open filter. The Firefly values resulted in radiance units of about 1×10^8-1×10^{10}, while bacterial values were 1×10^5-1×10^7, therefore the contribution of bacterial luciferase to mammalian luciferase values was negligible. Both bacterial luciferase (luxCDABE) and mammalian luciferase (Firefly) can be imaged using this method. Both bacterial and mammalian measurements

were compared to pre-injection values. Wet food was given to mice post-bacterial injection, and cage changes were performed daily.

Gemcitabine and ciprofloxacin administration

Gemcitabine (USP) was administered intraperitoneally (150 mg/kg), typically, on days 0, 4, and 9. Wet food was administered post-gemcitabine administration. The antibiotic ciprofloxacin was prepared at a concentration of 150mg/kg in 100µl sterile PBS, and was administered intraperitoneally, every 12 hours, from day 0 to day 6.

Clinical samples

Fresh samples of pancreatic tumors and normal pancreatic tissue were collected from patients with pancreatic ductal adenocarcinoma and from organ donors, respectively. The patients were treated at Massachusetts General Hospital, Boston USA or at the Sheba Medical Center, Israel. Tumor samples were collected and analyzed according to IRB-approved protocols.

DNA extraction

After weighing each collected tissue sample, DNA was extracted from each sample according to the protocol specified by the Mo-Bio UltraClean Tissue DNA Kit (#12334-50). This protocol involves a bead beating step to ensure full recovery of bacterial DNA. DNA concentration and quality were measured using the Nanodrop ND-1000. For negative controls the same protocol was applied to empty tubes.

Real-time quantitative polymerase chain reaction (qPCR) for bacteria

The following bacterial primers for the V6 region of the 16S ribosomal DNA (rDNA) region were used in combination: 5'-CNACGCGAAGAACCTTANC-3', 5'-ATACGCGARGAACCTTACC-3', 5'-CTAACCGANGAACCTYACC-3', 5'-CAACGCGMARAACCTTACC-3', 5'-CGACRRCCATGCANCACCT-3'.

DNA (150ng/well) extracted from tissues was combined with 500nM of the above described primer mix and 1X SYBR Green Master Mix (Qiagen QuantiTect SYBR Green PCR Kit #204143). The qPCR reaction was performed on the Applied Biosystems qPCR Sequence Detection System (#2900HT) at 50^{o}C for 2 min, 94^{o}C for 15 min to denature DNA, with amplification proceeding for 35 cycles at 94^{o}C for 15 s, 50^{o}C for 30 s, 72^{o}C for 30 s, and completed with a dissociation curve. Raw threshold cycle (C_t) values were compared to a bacterial standard curve produced with *Escherichia coli* DNA for approximation of bacterial load (fig. S13). To determine the presence of bacteria in each sample, the natural log was calculated for each qPCR result, which resulted in a normal distribution of the 41 DNA-free controls (as verified by the Kolmogorov-Smirnov test) (table S6). To reach a false positive rate of 0.1%, the cutoff was set to 10.5 bacteria/sample, which is equivalent to a Z-score of 3.1. The Wilcoxon Rank-Sum test was used to demonstrate that patients who underwent Endoscopic Retrograde Cholangiopancreatography (ERCP) had statistically more bacteria than patients who did not undergo ERCP.

Bacterial 16S rRNA fluorescence in situ hybridization (FISH)

Ribosomal RNA FISH was performed for the visualization of bacteria in human pancreatic tumor tissue. The protocol was adapted from Lyubimova et al. (*15*) and optimized for formalin-fixed paraffin-embedded (FFPE) tissues. We designed a set of 20 probes complementary to the 16S rRNA region that have broad coverage of bacterial species: 5'-ACTTGCATGTATTAGGCACG-3',
5'-GATGATTTGACGTCATCCCC-3', 5'-CTGAGCCAGGATCAAACTCT-3',
5'-TACGCATTTCACCGCTACAC-3', 5'-CAGGGTATCTAATCCTGTTT-3',
5'-CTACCTTGTTACGACTTCAC-3', 5'-ATCGTTTACGGCGTGGACTA-3',
5'-TATCTAATCCTGTTTGCTCC-3', 5'-TTTACGGCGTGGACTACCAG-3',
5'-CATTGTAGCACGTGTGTAGC-3', 5'-TCGACTTGCATGTGTTAAGC-3',
5'-CGACTTGCATGTGTTAAGCA-3', 5'-CATTGTGCAATATTCCCCAC-3',
5'-AGGGTATCTAATCCTGTTCG-3', 5'-GATATCTACGCATTTCACCG-3',
5'-CATGAGGACTTGACGTCATC-3', 5'-TAAGCATTCTGTCAGCGTTC-3',
5'-CACCTCTACACTTGTAGTTC-3', 5'-CGGCATTCCTACAAATATCT-3',
5'-CATTGTCCAATATTCCCCAC-3'

These 16S rRNA probes were labeled with the Cy5 fluorophore (GE Healthcare #PA25001). A set of 20 scrambled 16S rRNA probes based on the above described set was designed and also labeled with the Cy5 fluorophore. The scrambled probe sequences are as follows:
5'-TGTCAGCTTAGTCGAAACGT-3', 5'-GAACCGAGTGATTCCCTCTT-3',
5'-AACTGCGCTGATAACTACCG -3', 5'-TAACCTTTCCCATGACGCAC -3',
5'-TTAGTAGTCCTCTAGGTTCA -3', 5'- TGCCCTCACTGTTATACCAT-3',
5'-CGCTTGAACGTAATGCGGTT -3', 5'-TTGTATCTCTCTCACTCGTA -3',
5'-CAGCGGCCGTATGTATTACG -3', 5'-GTACTTGGTTGACCAGCGTA -3',
5'-TAGCTATAGCCTATTGGGCT -3', 5'-AGGCCTTTTACTAGGCATAG -3',
5'-CCTATAGTAGATCTCCTACC -3', 5'-CACGAATTTGTGGCTTGCAT-3',
5'-CCTCTGTACTACACGATAGT -3', 5'-TAACGGGCGCATCTGTCATA -3',
5'-TGTCTTCTTAGACAGTGCAC -3', 5'-CTATTCATACTTCCGCTGAC -3',
5'-CATCTCGCCCAATTAATATG -3', 5'-CCTATACTAGATCTCCTACC -3'.

Goblet cell probes (PMCID: PMC5293156) labeled with 6-Carboxytetramethylrhodamine (6-TAMRA) (ThermoFisher Scientific C6123) were obtained as a gift from Dr. Shalev Itzkovitz' lab at the Weizmann Institute of Science, and used as a control for the hybridization protocol in fig. S14. FFPE blocks were cut into 5µm slices and deparaffinized by immersing slides in 100% xylene for 10 min, followed by fresh 100% xylene for 5 min, 100% ethanol for 10 min, fresh 100% ethanol for 10 min, 95% ethanol for 10 min, and finally in 70% ethanol, and kept at 4˚C for a minimum of 2 hours. They were subsequently incubated in 2X SSC buffer (Ambion #AM9765) for 10 min at RT, then treated with 10 µg/ml proteinase-K (Ambion #AM2546) for 10 min at RT. Following proteinase-K treatment, samples were incubated twice with 2X SSC buffer for 5 min at RT, rinsed with a wash buffer containing 25% formamide (Ambion #AM9342), 2X SSC buffer, and nuclease-free water, then incubated with fresh wash buffer for an additional 5 min at RT. Probes were hybridized to the tissue overnight at 30˚C, using a hybridization buffer (300µl/slide) containing 25% formamide, 10% dextran sulfate (Sigma #D8906), 1 mg/ml *E. coli* tRNA (Sigma #R4251), 2X SSC buffer, 0.02% BSA (Ambion #AM2616), and nuclease-free water. Unbound probes were removed by

incubating samples in wash buffer for 30 min at 30˚C. Nuclear staining was performed by incubation with 25 ng/ml DAPI (Sigma #D9564) for 30 min at 30˚C. Samples were then placed in a GLOX buffer containing 1M TRIS (pH8 Ambion #AM9856), 2X SSC, 10% glucose, and nuclease-free water for 5 min at RT, before being mounted onto slides with an anti-bleach mounting medium containing GLOX buffer, 37 µg/ml glucose oxidase (Sigma G2133), and 0.29 mg/ml Catalase suspension (Sigma #3515). Slides were imaged at 100X or 60X magnification, using an inverted epifluorescent microscope. Exposure time was 1 s for the Cy5 fluorescence channel, 1 s for the Alexa Fluor 594 fluorescence channel, 1 s for the TMR fluorescence channel, and 50 ms for the DAPI fluorescence channel. To discard nonspecific fluorescence background, for some of the images (Fig. 4B), the fluorescence signal from the Alexa Fluor 594 channel was subtracted from the Cy5 channel using ImageJ. Please note that as pancreatic tissue contains large amounts of RNAses it is imperative to fix small tumor samples very quickly to best preserve the RNA.

Immunohistochemistry for bacterial lipopolysaccharide (LPS) in human pancreatic tumors

Immunohistochemistry was performed on 4 µm serial sections from formalin-fixed, paraffin-embedded (FFPE) tissues. The samples were deparaffinized, rehydrated, and pretreated for antigen retrieval by microwave treatment for 10 min in 10 mmol/l of citrate buffer (pH 6.0). Endogenous peroxidase was quenched by incubating samples with 0.3% hydrogen peroxide in PBS for 30 min. To detect gram-negative bacteria, antibody to Lipopolysaccharide core (Hycult Biotech, Uden, Netherlands; Clone WN1 222-5) was used at a concentration of 1:300 overnight at 4˚C. ZytoChem Plus HRP Polymer Anti-Rabbit secondary antibody was used, according to the manufacturer's instructions (Zytomed Systems, Berlin, Germany). DAB substrate Kit was used to detect HRP (Zytomed Systems, Berlin, Germany), and specimens were counterstained with hematoxylin.

16S rRNA amplification and sequencing

A total of 65 PDAC samples were subjected to 16S rDNA sequencing. Twenty-seven of these samples originated in the USA and 38 in Israel. For the samples obtained in the USA, the 16S gene dataset consists of Illumina MiSeq sequences targeting the V4 variable region. Detailed protocols used for 16S amplification and sequencing were previously described (*24*). In brief, genomic DNA was subjected to 16S amplification using primers designed to incorporate the Illumina adapters and a sample barcode sequence, allowing for directional sequencing covering variable region V4 (Primers: 515F [5'-GTGCCAGCMGCCGCGGTAA-3'] and 806R [5'-GGACTACHVGGGTWTCTAAT-3']). PCR reactions contained 10 µl of diluted template (1:50), 10 µl of HotMasterMix with the HotMaster Taq DNA Polymerase (5 Prime), and 5 µl of primer mix (2 µM of each primer). The cycling conditions consisted of an initial denaturation at 94°C for 3 min, followed by 30 cycles of denaturation at 94°C for 45 s, annealing at 50°C for 60 s, extension at 72°C for 5 min, and a final extension at 72°C for 10 min. Amplicons were quantified on the Caliper LabChipGX (PerkinElmer, Waltham, MA), pooled in equimolar concentrations, size selected (375-425 bp) on the Pippin Prep (Sage Sciences, Beverly, MA) to reduce non-specific amplification products from host DNA, and a final library size and quantification was

performed on an Agilent Bioanalyzer 2100 DNA 1000 chips (Agilent Technologies, Santa Clara, CA). Sequencing was performed on the Illumina MiSeq platform (version 2), according to the manufacturer's specifications, with the addition of 5% PhiX, and it generated paired-end reads of 175 bases in length in each direction. The overlapping paired-end reads were stitched together (approximately 97 bp overlap), size-selected to reduce non-specific amplification products from host DNA (225-275 bp), and further processed in a data curation pipeline implemented in QIIME 1.7.0 as pick_closed_reference_otus.py (*25*). In brief, this pipeline uses a reference-based method to pick operational taxonomic units (OTUs), and constructs an OTU table. Taxonomy was assigned using the Greengenes (August, 2013) predefined taxonomy map of reference sequence OTUs to taxonomy (*26*). For the samples originating in Israel, we used a novel method which amplifies 5 regions across the 16S rDNA gene to allow for better species resolution. The method will be reported in detail elsewhere. The resulting OTU tables of both datasets were checked for mislabeling (*27*) and contamination (*28*). A mean sequence depth of 73,095 reads/sample was obtained for all 65 samples. For the final analysis, tumor samples (N=65) were compared to DNA extraction or PCR technical controls (N=35). Species that were absent across all control samples were all considered in further analysis. For all other species that had some presence in the control samples, a p-value indicating abundance in tumors compared to controls was calculated based on a binomial distribution (proportion was given by the frequency of positive control samples). Species that passed a Benjamini-Hochberg false discovery rate of 5% were considered for the final analysis.

Culturing bacteria from human PDAC samples

Fresh tumor tissue (around 3-5mm^3) or 50µl of sterile PBS (negative control) was placed in 1 ml of LB broth and cultured overnight at 37˚C while shaking. In the morning, LB from overnight culture was diluted in serial 1:10 dilutions to obtain single colonies on LB agar plates (without antibiotics). Once bacterial colonies appeared (usually after 1-3 days of incubation), they were grown individually in LB and stored.

PCR and Sanger sequencing of 16S from single bacterial colonies

The following forward and reverse bacterial primers, respectively, for the V1-V9 16S rRNA regions, were used for PCR: 5' AGRGTTTGATCMTGGCTCAG 3', 5' TACGGYTACCTTGTTAYGACTT 3'. The DDW, buffer, dNTPs, $MgCl_2$ and Taq were obtained from the Platinum® Taq DNA Polymerase High Fidelity kit (#11304-011).
PCR reactions contained 40.8 µl of PCR DDW, 5 µl of buffer X10, 1 µl of 10mM dNTPs, 2 µl of 50mM $MgSO_4$, 0.2 µl of Platinum® Taq HF, and 0.5 µl of both the forward and reverse primers (final concentration of 20 µM). DNA was added by touching a bacterial colony from an LB agar plate with a tip. Reactions were held at 96°C for 5 min to denature the DNA, with amplification proceeding for 30 cycles at 94°C for 30 s, 57°C for 60 s, and 72°C for 2 min, with a final extension of 7 min at 72°C to ensure complete amplification.
The PCR product was run on a DNA separating gel, and the single band (~1465 bp) was cleaned with the Qiagen - QIAquick PCR Purification Kit (#28104). The PCR product was sent to sequencing, using the following primers:
27f - 5' AGRGTTTGATCMTGGCTCAG 3', 926r - 5' CCGTCAATTCMTTTRAGT 3', 1492r - 5' TACGGYTACCTTGTTAYGACTT 3'. Sequencing results were aligned to the

16S Ribosomal RNA Sequences (Bacteria and Archaea) Database in the NCBI blastn site.

Bacteria-mediated resistance to gemcitabine by bacteria isolated from human pancreatic tumors

Bacteria from 15 pancreatic tumors were cultured in LB overnight, as described above. The next morning, bacteria were diluted 1:25 in DMEM and transferred into 96-well U-shaped plates (BD Falcon 353077). Gemcitabine was then added to bacteria at a final concentration of 80X (20uM), and incubated with the bacteria for 4 hours at 37^{o}C. To filter out the bacteria, the bacteria-drug mix was then diluted 1:8 into 96-well filter plates (Pall #8119), and centrifuged at 1500 × g for 10 min at RT into 96-well receiver plates (VWR #82051-242). The final filtrate was added to GFP-labeled RKO and HCT116 human colorectal carcinoma cells, resulting in a 1X concentration of 0.25uM gemcitabine on the cells. Cell growth was followed for 7 days by reading GFP fluorescence.

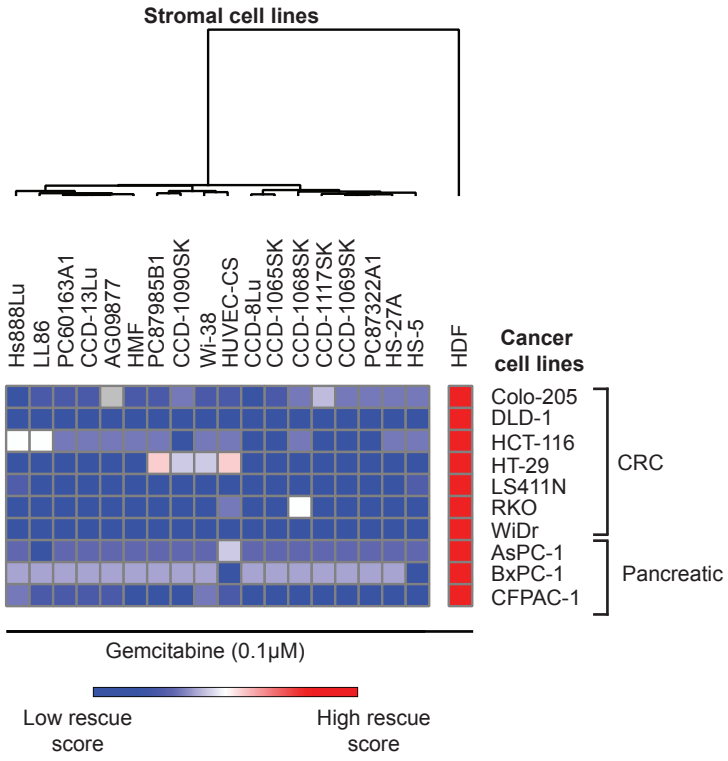

Fig. S1.
Hierarchical clustering of stromal cells (horizontal) according to their ability to confer gemcitabine resistance to colorectal (CRC) and pancreatic cancer cell lines (labeled in vertical panel). Red and blue colors represent row maximum and minimum rescue scores, respectively. This supplementary figure was copied from our previous publication *(5)*.

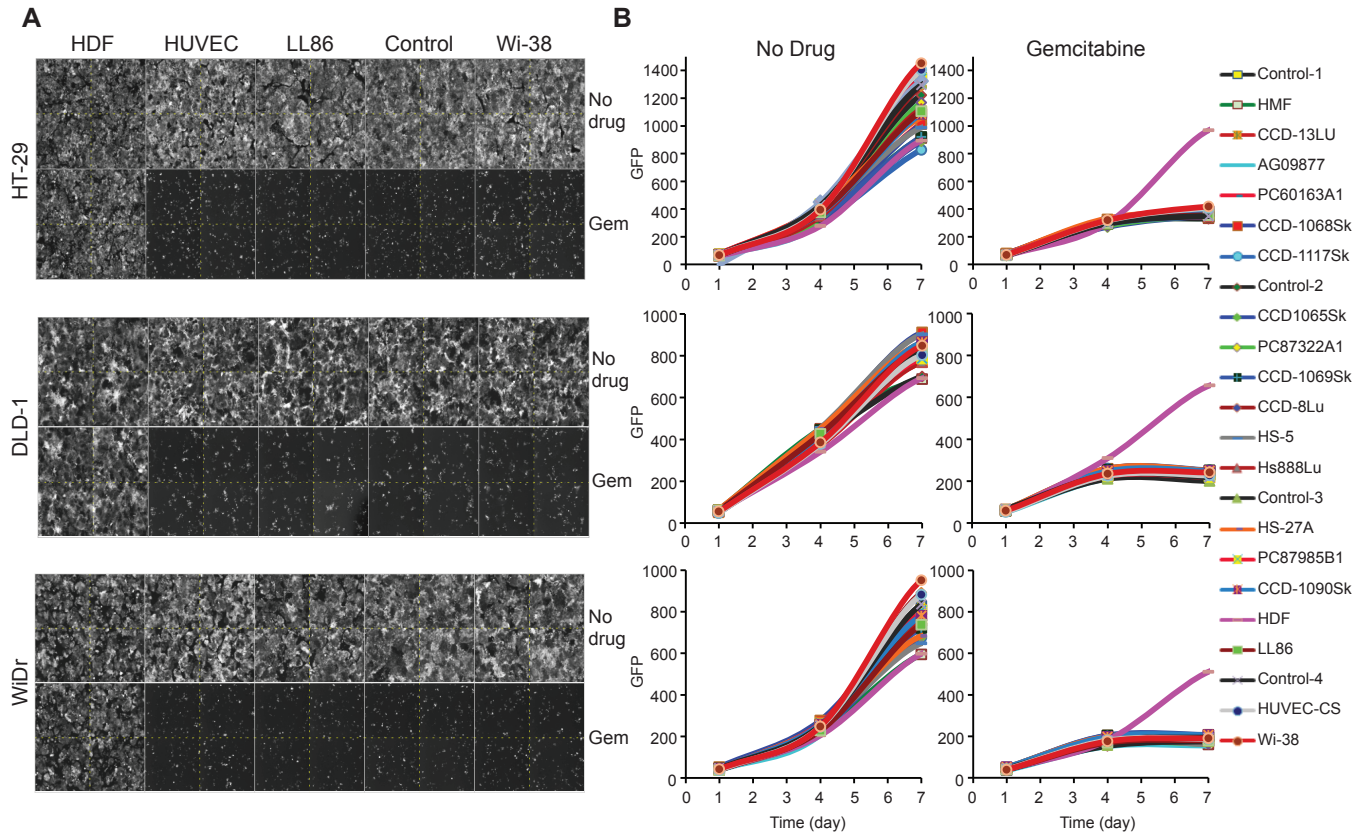

Fig. S2.
Rescue of colorectal cancer cells from gemcitabine (Gem) by HDF stromal cells. HT-29 was treated with 0.02 μM gemcitabine, whereas DLD-1 and RKO cells were treated with 0.1 μM gemcitabine. **(A)** Fluorescence microscopy looking at GFP positive cancer cells on day 7. All 4 quadruplicate wells are shown. **(B)** Growth curves of cancer cell lines. Colors represent the stromal cell that was co-cultured with the cancer cell line (control = no stromal cells). Since GFP was detected, only the growth of the cancer cells in the well was measured. This supplementary figure was copied from our previous publication *(5)*.

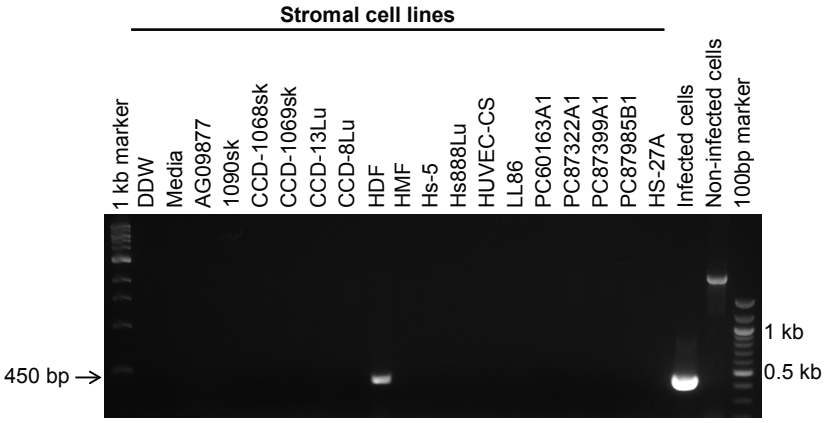

Fig. S3.
Mycoplasma infection was detected in HDF cells using *Mycoplasma*-specific PCR primers (supplementary methods).

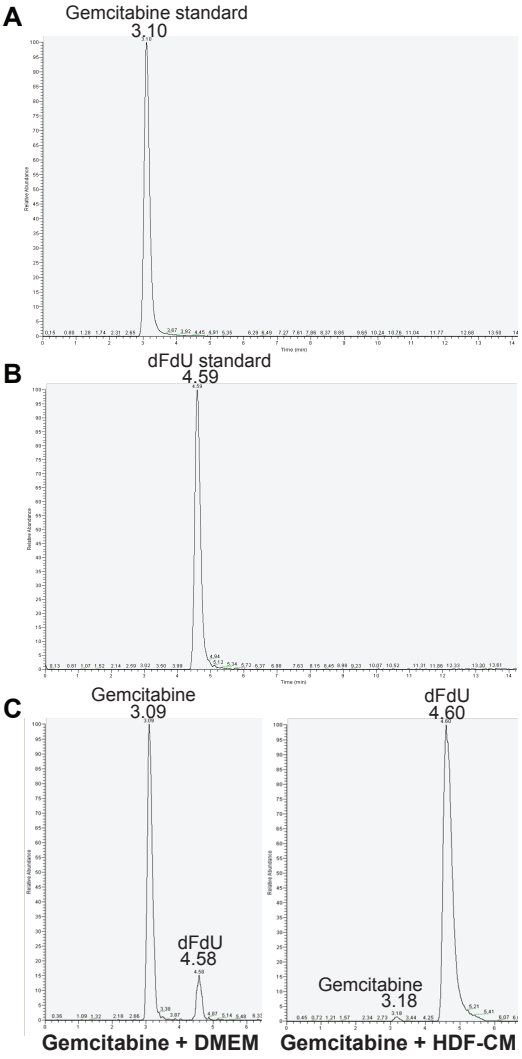

Fig. S4.
HDF-conditioned medium (HDF-CM) converts gemcitabine into 2' ,2'-difluorodeoxyuridine (dFdU). **(A)** HPLC-MS/MS of gemcitabine (100nM) standard. **(B)** HPLC-MS/MS of dFdU (100nM) standard. **(C)** HPLC-MS/MS of gemcitabine (100nM) incubated for 4 hours at 37˚C with HDF-CM or with DMEM medium control.

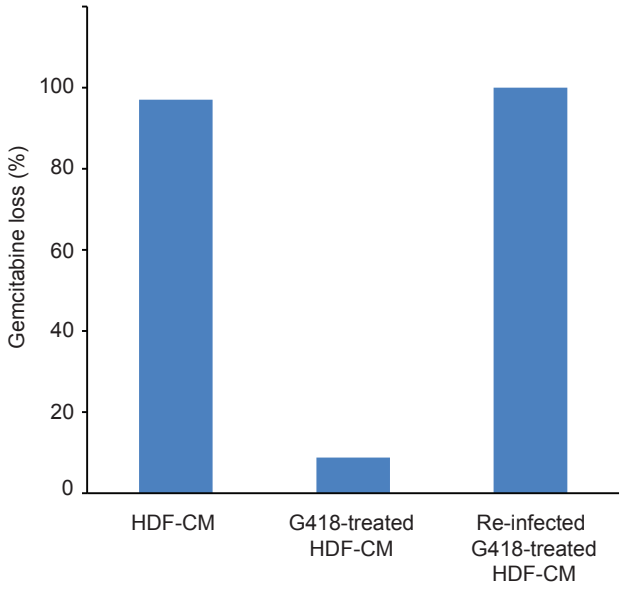

Fig. S5.
HDF-mediated metabolism of gemcitabine is dependent on *M. hyorhinis*. Gemcitabine (0.64µM) was incubated for 24 hours at 37˚C with HDF-CM (*M. hyorhinis* positive), HDF-CM from G418-treated HDF cells (*M. hyorhinis* negative), or HDF-CM from G418-treated cells after re-infection with *M. hyorhinis*. HPLC-MS/MS was used to detect the percentage of gemcitabine loss after 24 hours, compared to pre-incubation gemcitabine levels.

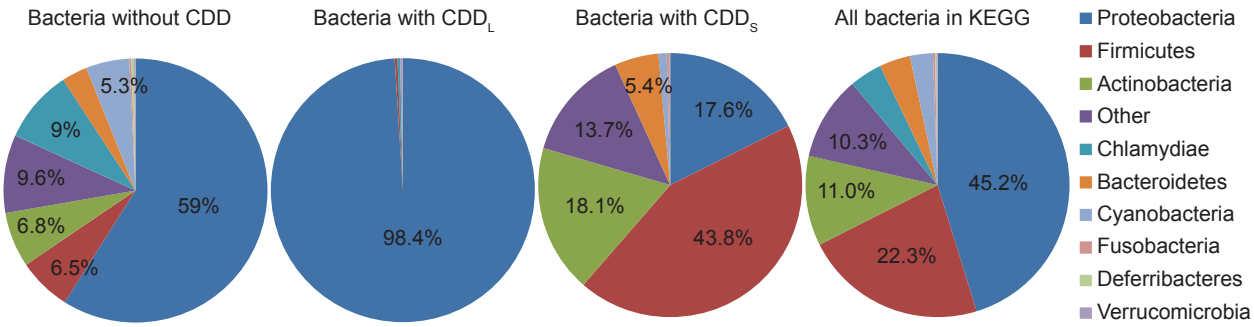

Fig. S6.
Distribution of bacterial phyla by CDD status. 2,674 bacteria in the Kyoto Encyclopedia of Genes and Genomes (KEGG) were classified, based on their CDD isoform, into bacteria without CDD, bacteria with the long CDD isoform (CDD$_L$), and bacteria with the short CDD isoform (CDD$_S$) (see table S5 for more details). As shown, 98.4% of bacteria with the CDD$_L$ isoform belong to the Proteobacteria phylum.

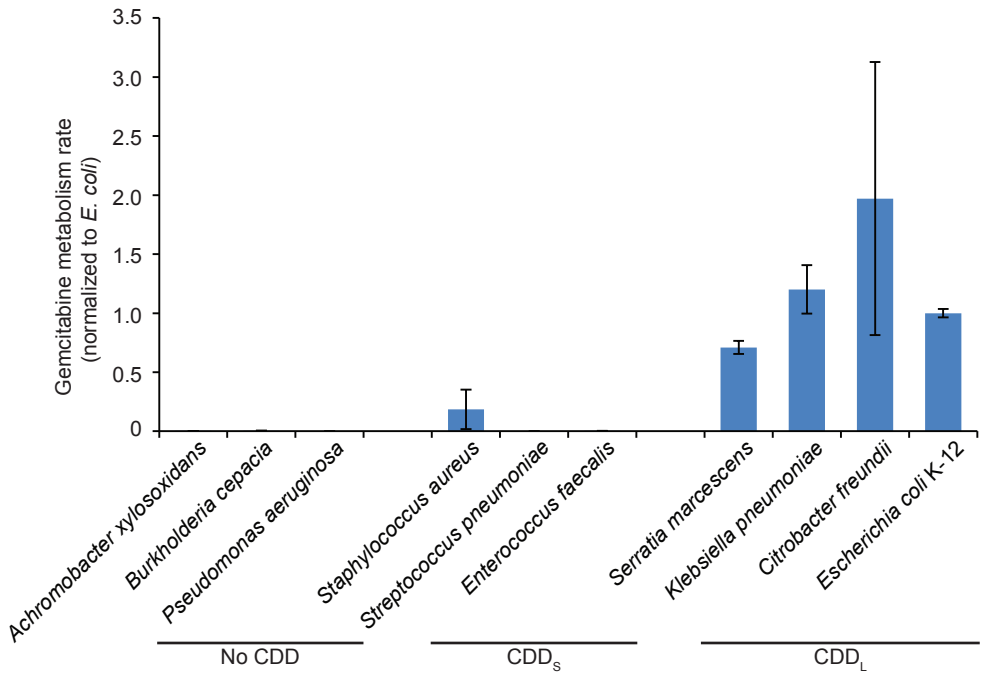

Fig. S7.
Rate of gemcitabine metabolism by bacteria with different CDD isoforms. Gemcitabine (4 μM) was incubated with 10^7 bacteria for 4 hours in M9 Minimal Salts medium (Sigma, M9956-500ML) to keep the number of bacteria constant throughout incubation. Bacteria were then filtered from the media, and the remaining gemcitabine was detected by HPLC-MS/MS. All CDD_L bacteria were isolated from PDAC tumors, excluding *E. coli*. Bars represent the standard deviation between 2 biological replicates, each containing 2 technical repeats.

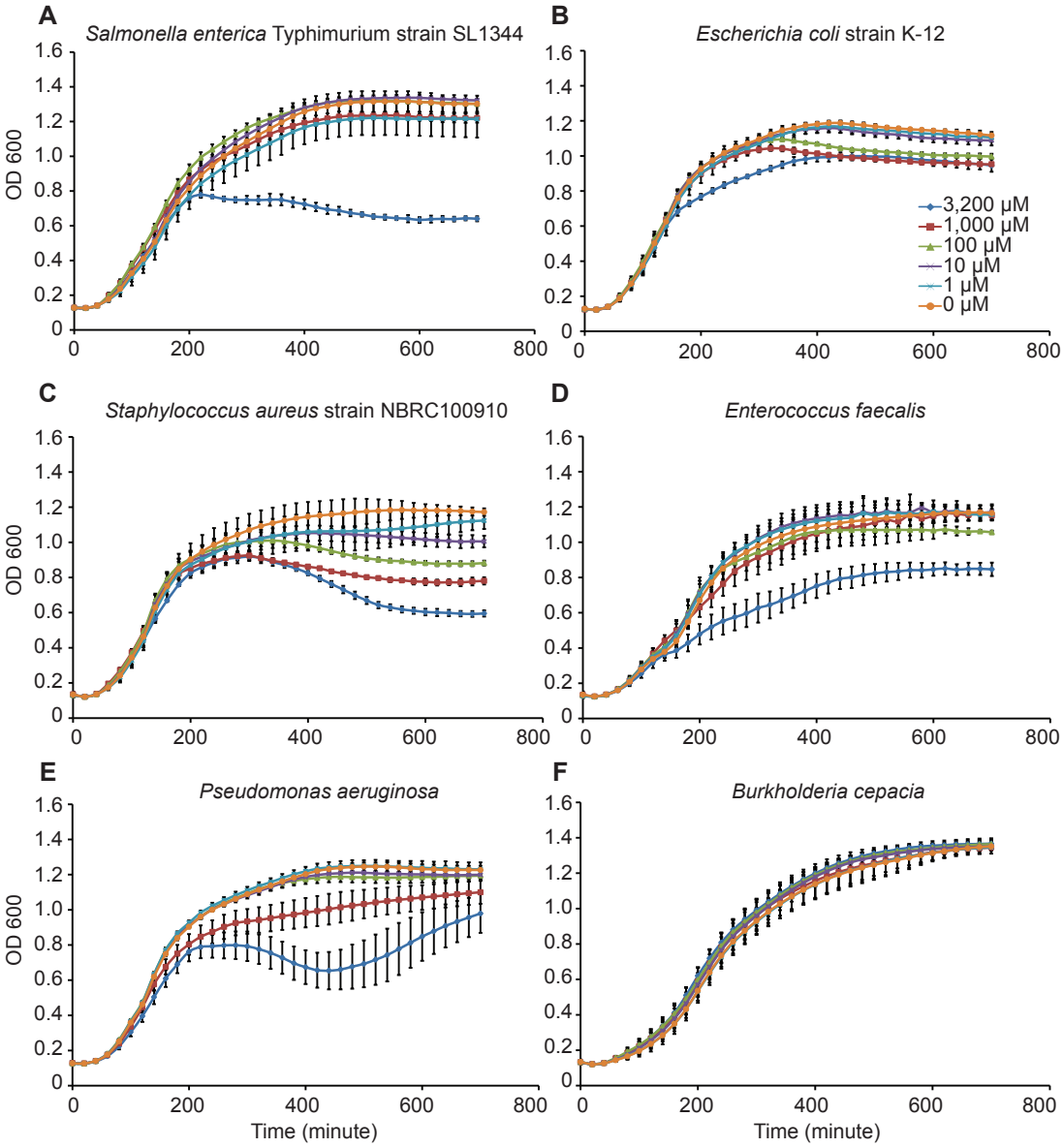

Fig. S8.

The effect of gemcitabine on bacterial growth. Overnight bacterial cultures were diluted to $5x10^6$ bacteria/well, and gemcitabine was added (0-3,200 µM) to each well. OD 600 measurements were used to detect bacterial growth. **(A,B)** Bacteria containing CDD_L. **(C,D)** Bacteria containing CDD_S. **(E,F)** Bacteria lacking CDD. Bars represent the standard deviation between 2 biological replicates, each containing 3 technical repeats.

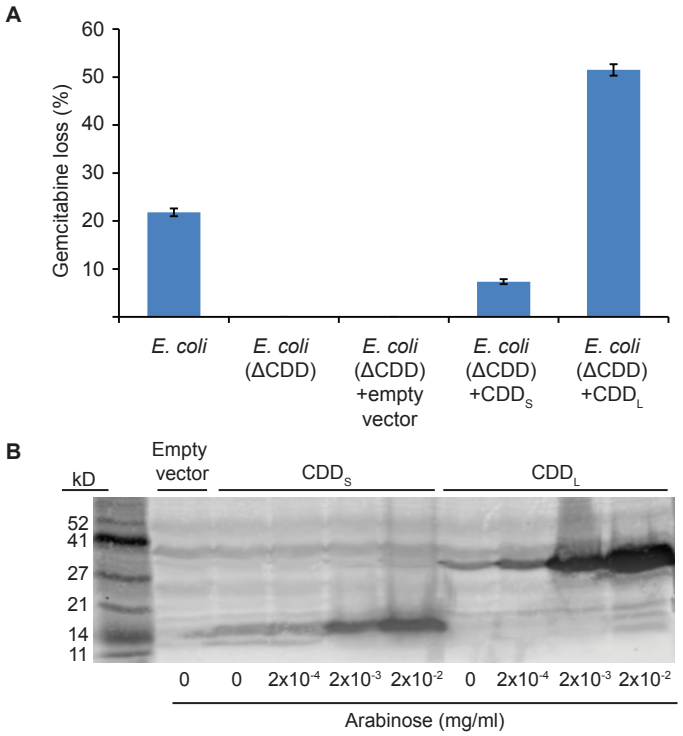

Fig. S9.
Effect of complementing *E. coli* ΔCDD with CDD_S or CDD_L on metabolism of gemcitabine. FLAG-tagged sequences of CDD_S or CDD_L, originating from *Staphylococcus aureus* or *Shigella flexneri* (note that the CDD_L protein sequence of *S. flexneri* is identical to that of *E. coli* K-12), respectively, were cloned into the pBAD/HisA vector containing an arabinose-inducible promoter. These cloned plasmids, or the empty vector, were then transformed into the *E. coli* ΔCDD strain. **(A)** 40 μM gemcitabine was incubated with 10^7 bacteria for 4 hours at 37˚C in M9 Minimal Salts medium (Sigma, M9956-500ML) to keep the number of bacteria constant throughout incubation. For CDD expression, arabinose was added at a concentration of $2x10^{-3}$ for CDD_S and $2x10^{-4}$ mg/ml for CDD_L. Bacteria were then filtered from the media, and the remaining gemcitabine was detected by HPLC-MS/MS. Bars represent standard deviation between 2 technical repeats. **(B)** Western blot showing expression of CDD_S or CDD_L as detected by Anti-FLAG antibody (Sigma #f3165) and secondary Anti-Mouse IRDye680 antibody (Li-cor #926-68070).

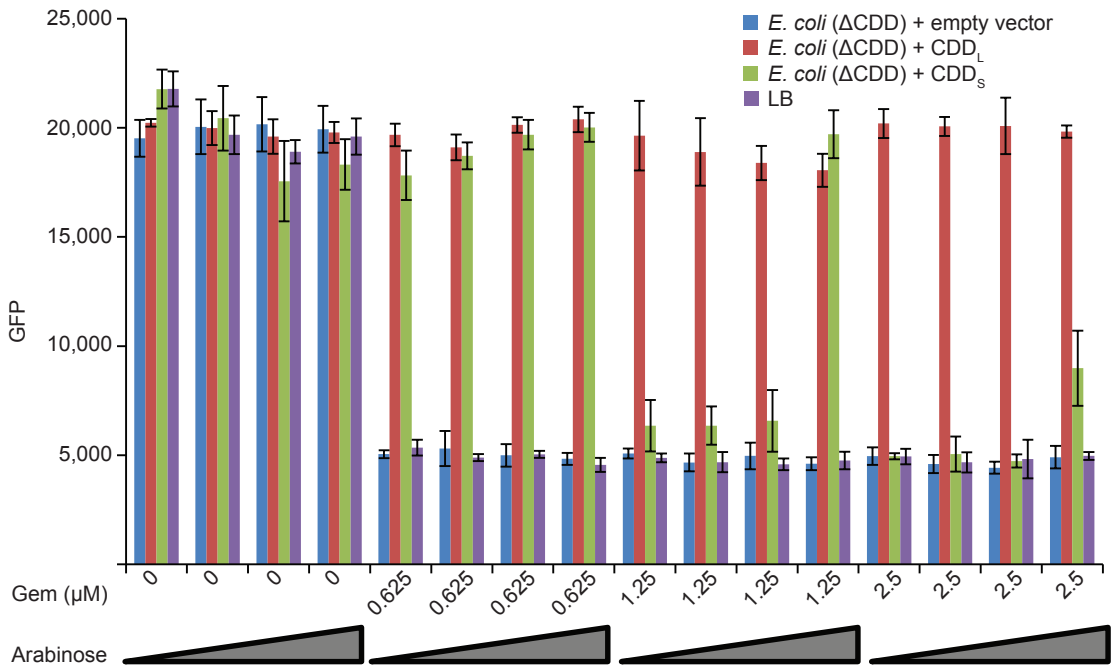

Fig. S10.
Effect of complementing *E. coli* ΔCDD with CDD_L or CDD_S on resistance of PDAC cell line (AsPC1) to gemcitabine. FLAG-tagged sequences of CDD_L or CDD_S originating from *Shigella flexneri* and *Staphylococcus aureus* respectively, were cloned into the pBAD/HisA vector containing an arabinose-inducible promoter. These cloned plasmids, or the empty vector, were transformed into the *E. coli* ΔCDD strain. Bacteria were diluted 1:25 from overnight culture into a well with DMEM containing gemcitabine (Gem) concentrated 80X the final concentration with which the AsPC1 cells were treated. Gemcitabine values on the x-axis represent the 1X concentration. Additionally, bacteria were treated with arabinose at increasing concentrations for expression of CDD (0 mg/ml, $2x10^{-4}$ mg/ml, $2x10^{-3}$ mg/ml, $2x10^{-2}$ mg/ml). After 4 hours of incubation at 37˚C, bacteria were filtered out, and GFP-positive AsPC1 cells were treated with this filtered medium. Medium was changed and cells retreated on day 4. GFP fluorescence was measured over 6 days to track cell growth. Values at day 6 were normalized by subtracting day 1 from day 6 (y-axis). Bars represent standard deviation between 4 technical repeats.

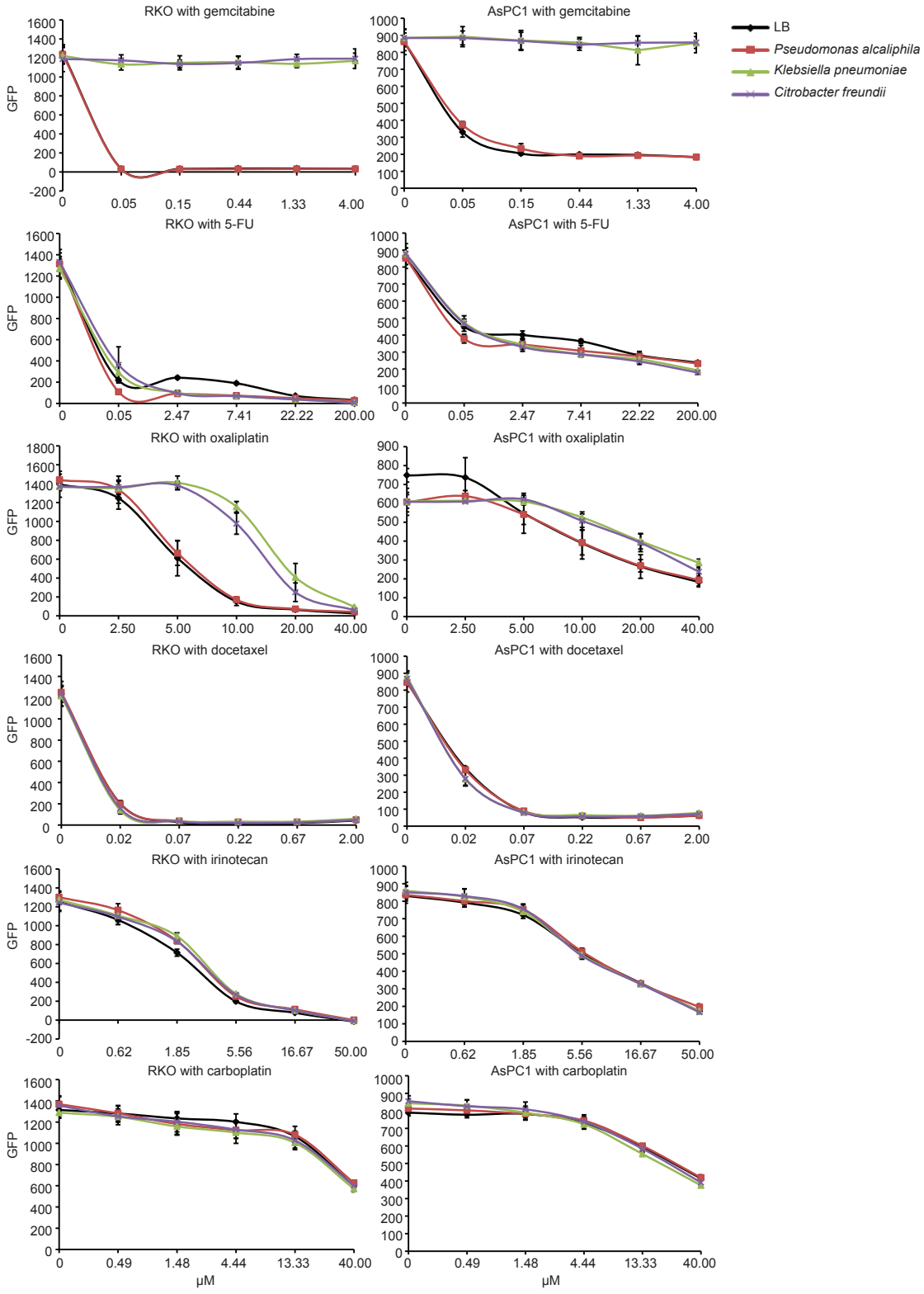

Fig. S11.

Bacteria can mediate resistance to oxaliplatin. Bacteria were incubated with drugs for 4 hours in DMEM at 37˚C, after which they were filtered out, and this filtered medium was added to GFP-labeled AsPC1 or RKO cells. Results presented are GFP fluorescence reads from day 7 of the experiment. Two bacterial species shifted the dose response curve to the right for both gemcitabine and

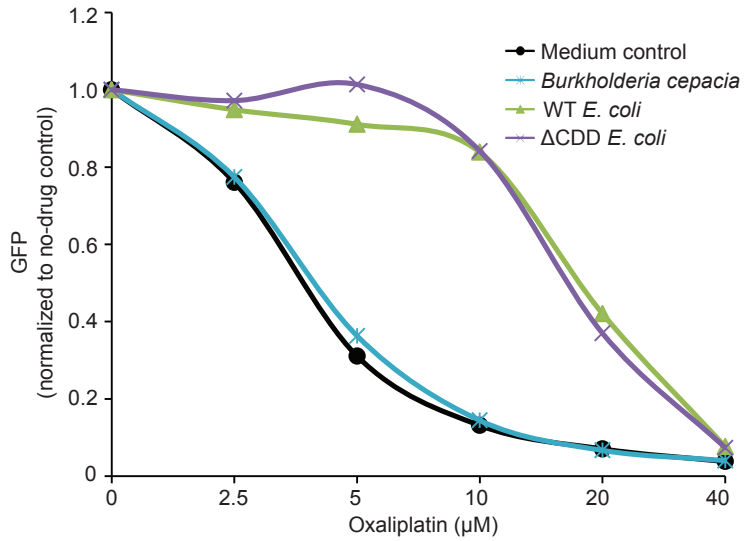

Fig. S12.
CDD does not mediate resistance to oxaliplatin. Oxaliplatin was incubated with different bacteria (or with bacteria-free medium control) for 4 hours in DMEM at 37˚C. Bacteria were then filtered out, and the filtered media were added to GFP-labeled RKO colon cancer cells. GFP fluorescence reads at day 7 were normalized to the no-drug control. Both WT *E. coli* and ΔCDD *E. coli* conferred resistance to oxaliplatin to the same extent.

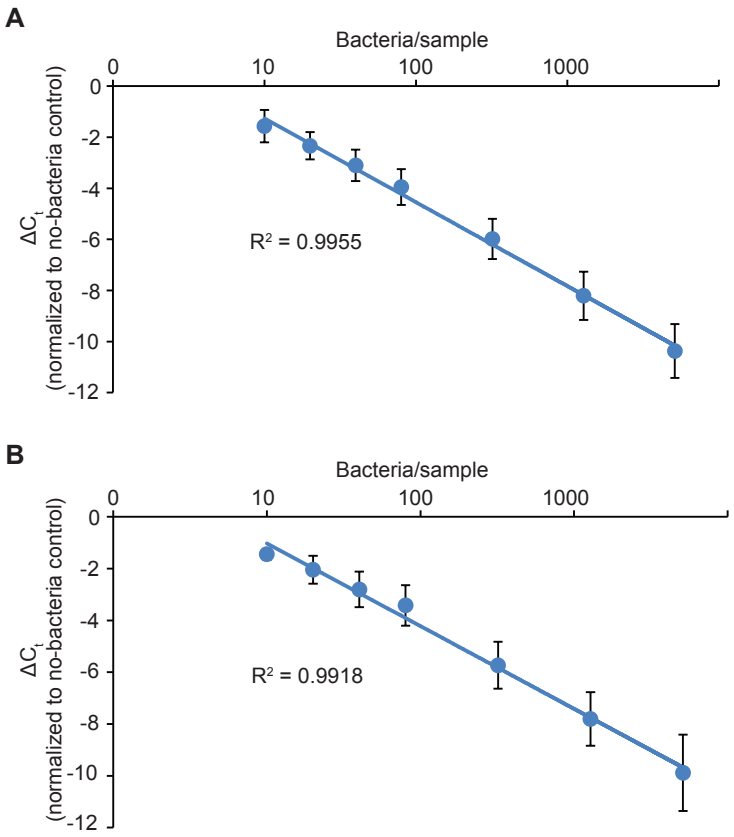

Fig. S13.
Estimating the number of bacteria by bacterial 16S rDNA qPCR. **(A)** Increasing amounts of *E. coli* bacterial DNA (equivalent to 0-5,120 bacterial cells) were spiked into 150 ng of human DNA, then subjected to qPCR for 16S rDNA. **(B)** *E. coli* cells (0-5,120 bacterial cells) were spiked into human AsPC1 cells (equivalent to 150 ng DNA) before DNA extraction. After DNA extraction, these samples were subjected to qPCR for 16S rDNA. 0.005pg of bacterial DNA was considered to be equivalent to 1 bacterium, and 6.2 pg of human cell DNA was considered to be equivalent to one AsPC1 cell. Bars represent the standard deviation between 3 biological replicates.

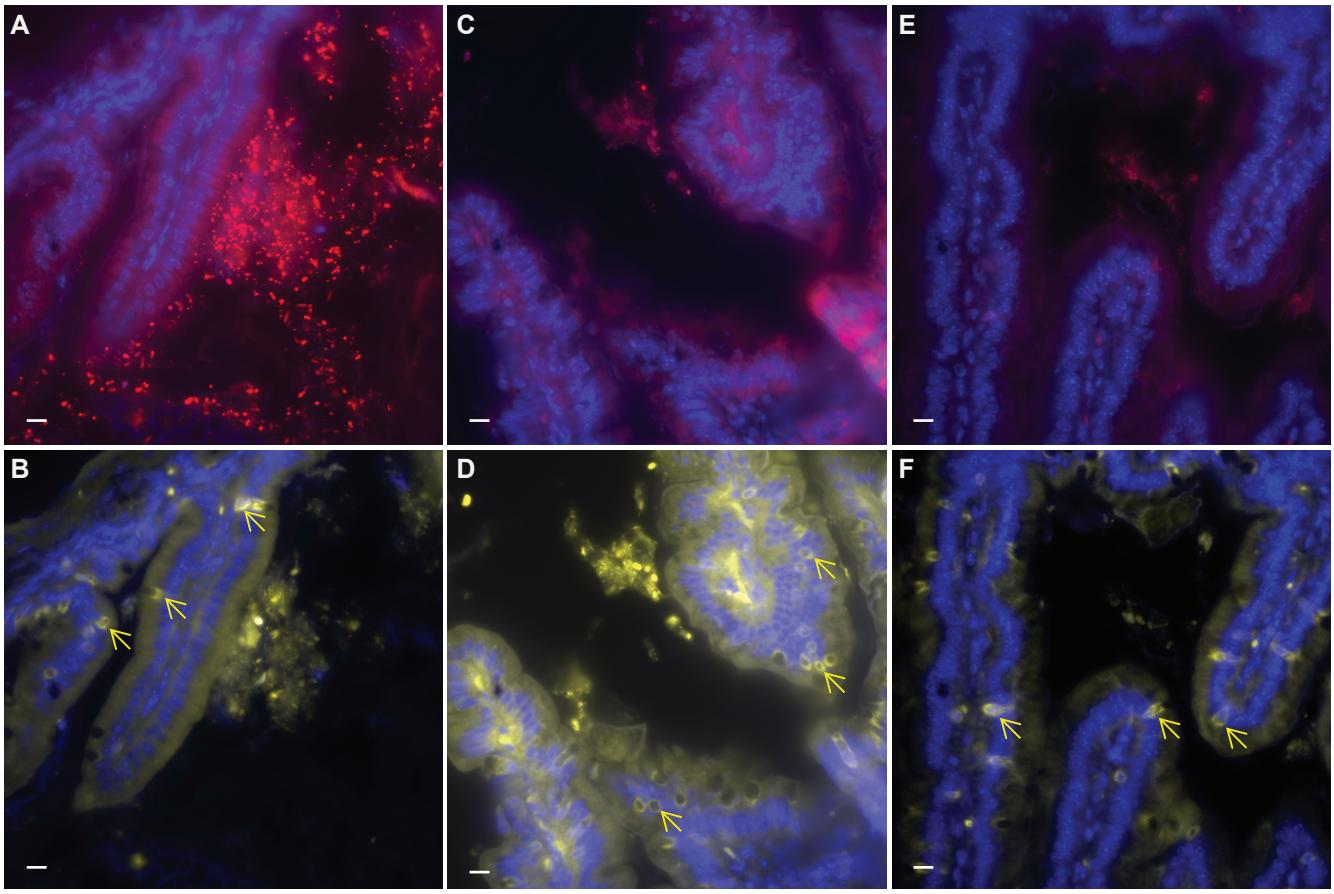

Fig. S14.
Controls for bacterial 16S rRNA fluorescence in situ hybridization probes. **(A)** Wild type mouse colon section hybridized with 16S rRNA probe (red) and DAPI (blue). **(B)** Same mouse colon section hybridized with goblet-cell marker (*Gob5)* (yellow) and DAPI (blue). The *Gob5* probe is used as a positive control for the fluorescence in situ hybridization protocol. Three goblet cells are marked by yellow arrows. **(C)** Germ-free mouse colon section hybridized with 16S rRNA probe (red), DAPI (blue), and **(D)** *Gob5* probe (yellow). **(E)** Wild type mouse colon section hybridized with scrambled 16S rRNA probe (red), DAPI (blue), and **(F)** *Gob5* probe (yellow). All fields imaged at 60X magnification. Scale bars, 10 μm.

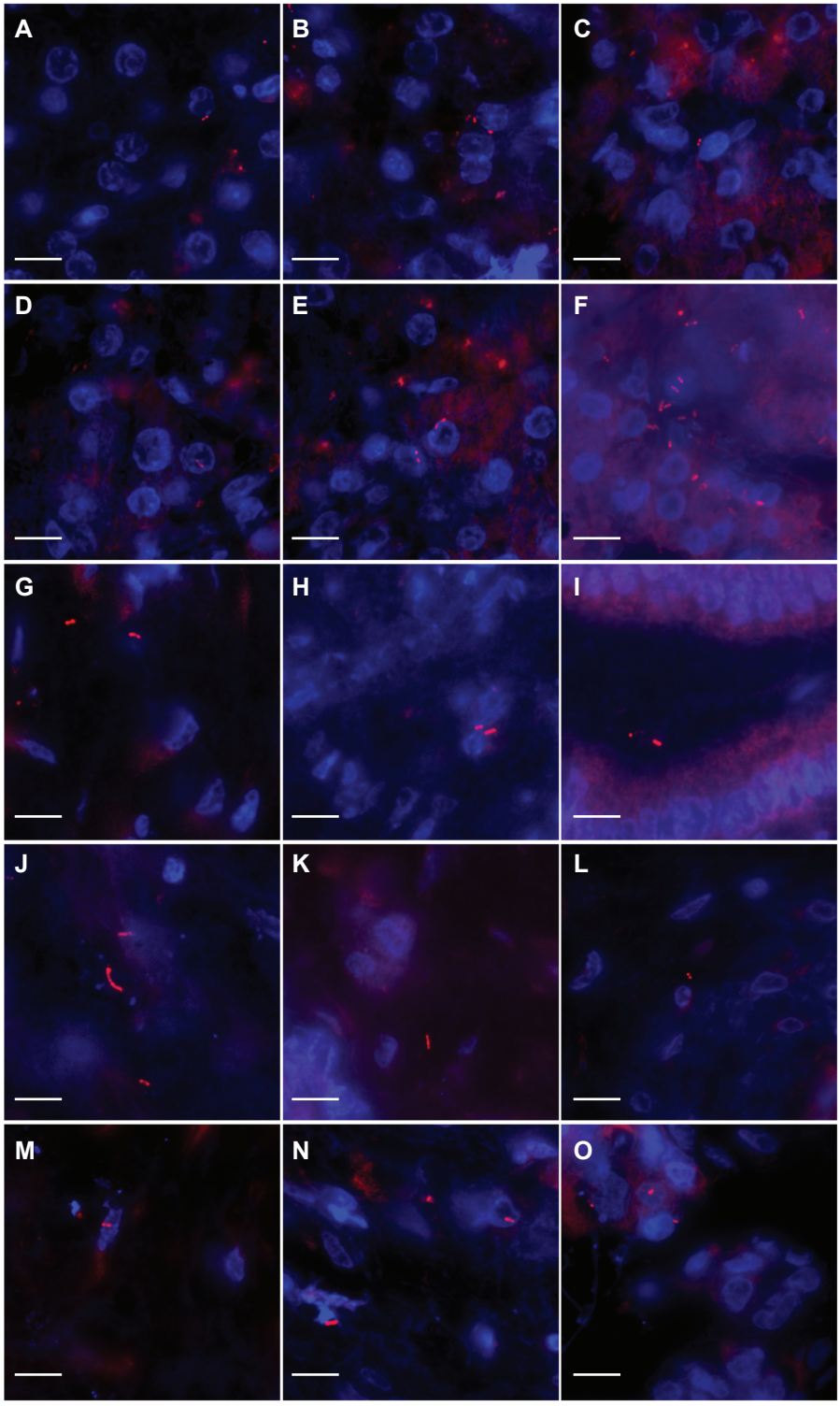

Fig. S15.
Bacteria detected by bacterial 16S rRNA fluorescence in situ hybridization probes in 5 PDAC patients. **(A-F)** Patient #1**. (G)** Patient #2. **(H-J)** Patient #3. **(K)** Patient #4. **(L-O)** Patient #5. All fields imaged at 100X magnification. Scale bars, 10 μm.

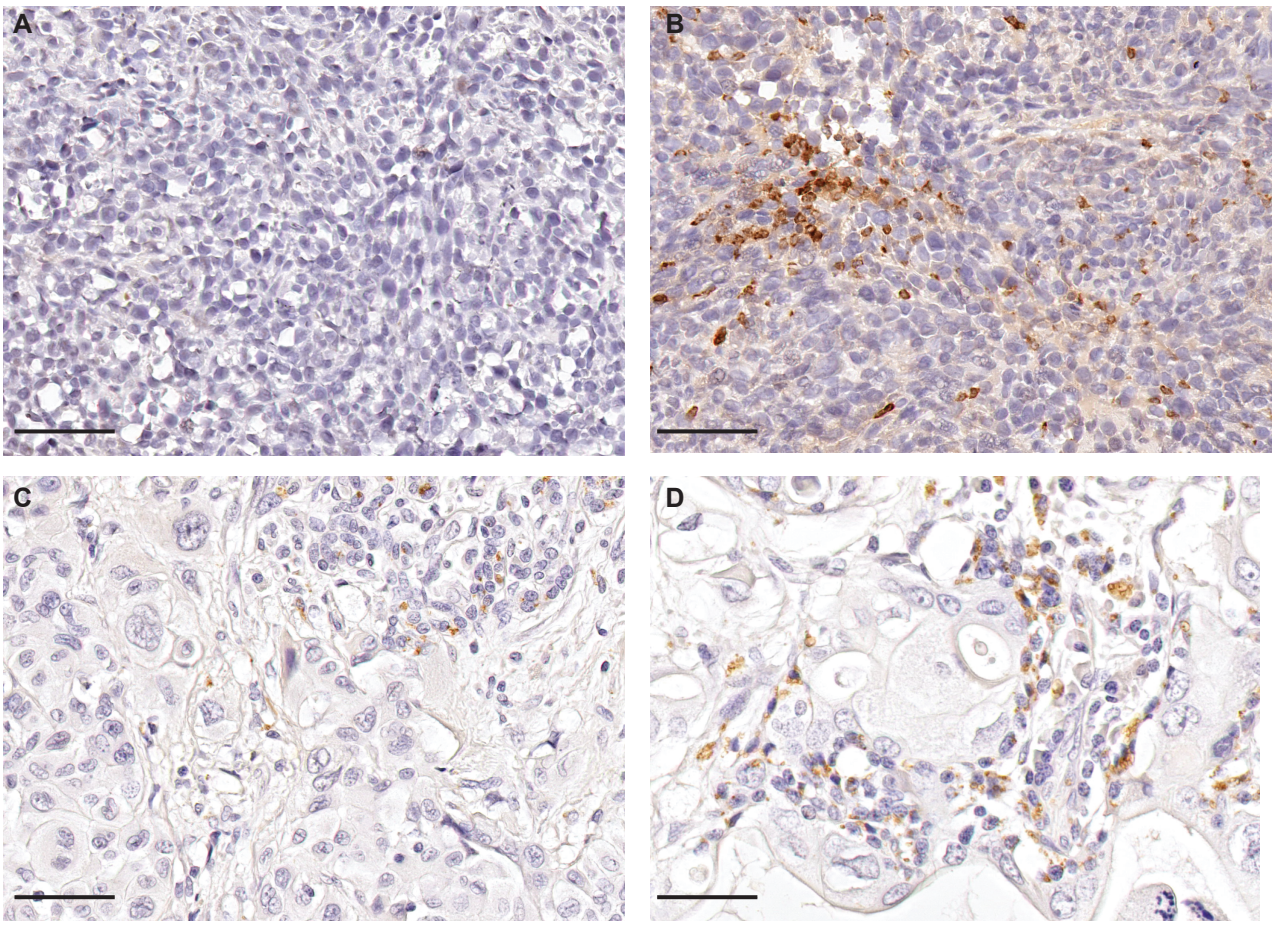

Fig. S16.
Detection of bacterial LPS by immunohistochemistry. MC-26 mouse colon cancer cells were injected subcutaneously into the flanks of BALB/c mice. After tumors reached 5-7mm in diameter, **(A)** PBS or **(B)** *E. coli* Nissle 1917 were injected into the tail vein. Seven days later, tumors were harvested, formalin fixed, and paraffin embedded. Slides from both tumors were subjected to IHC, using an anti-LPS antibody staining bacteria in brown. **(C,D)** Human PDAC tumors subjected to IHC, using an anti-LPS antibody. Scale bars, 50 μm.

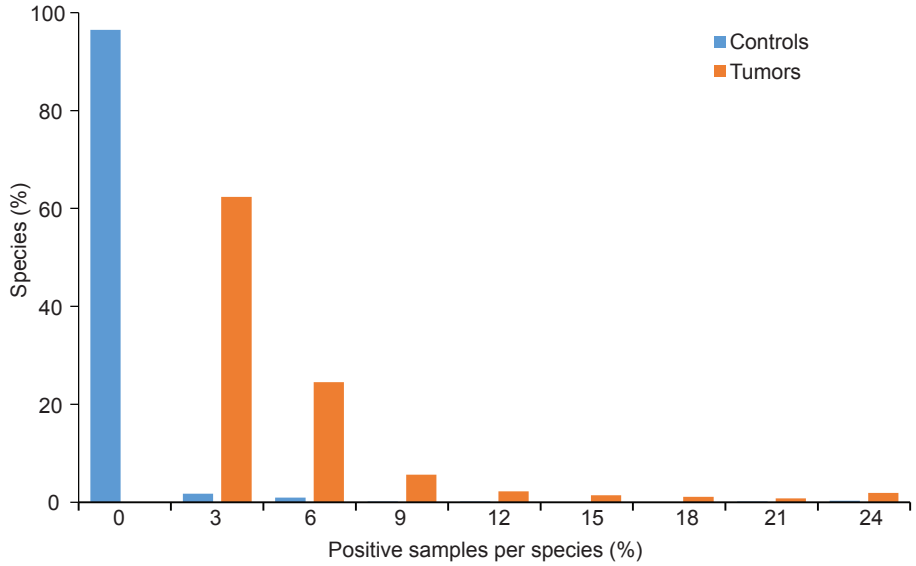

Fig. S17.
Histogram of bacterial species prevalence across tumor and control samples. 65 human PDAC samples and 35 negative controls were subjected to DNA extraction followed by 16S rDNA amplification and sequencing (supplementary methods). The graph depicts a histogram of the percentage of samples (tumors or controls) that were positive for each bacterial species.

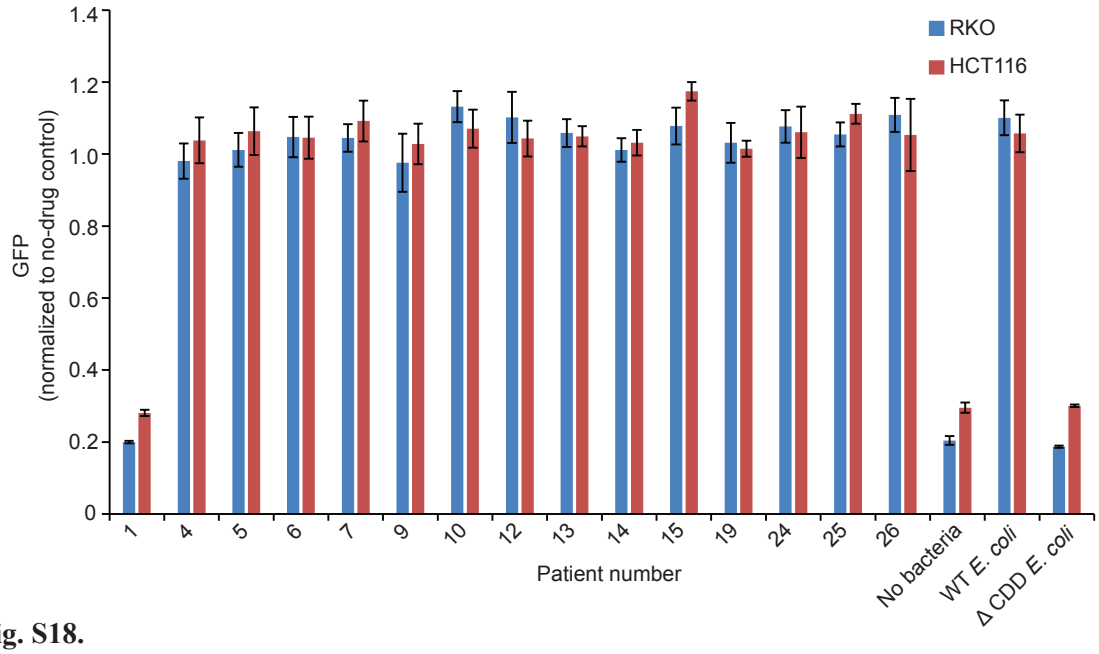

Fig. S18.
Bacteria-mediated resistance to gemcitabine by bacteria isolated from human pancreatic tumors. Bacteria from 15 pancreatic tumors were cultured overnight in LB. The next morning, bacteria were diluted 1:25 in DMEM, and gemcitabine was added. After 4 hours of incubation at 37˚C, bacteria were filtered out and this filtered medium was added to GFP-labeled RKO and HCT116 cancer cells. Cells were followed for 7 days by GFP fluorescence measurement. For specific details, see the supplementary methods. Note that bacteria were cultured in LB media and aerobic conditions, and thus selected against anaerobic bacteria or bacteria that cannot thrive in LB media.

Table S1A Cancer cell lines used in the study.
Table S1B Stromal cells used in the study.
Table S1C Bacteria used in the study.
Table S2 Identity of reads from whole genome sequencing of HDF conditioned media.
Table S3 CDD and bacteria-mediated gemcitabine resistance.
Table S4 Alignment of amino acid sequences from bacteria that harbor the short or long CDD gene.
Table S5 CDD in bacteria.
Table S6 16S qPCR results of pancreatic tumors and controls.
Table S7 16S sequencing results (% of reads).

References and Notes

1. F. Klemm, J. A. Joyce, Microenvironmental regulation of therapeutic response in cancer. *Trends Cell Biol.* **25**, 198–213 (2015). doi:10.1016/j.tcb.2014.11.006 Medline

2. S. L. Topalian, F. S. Hodi, J. R. Brahmer, S. N. Gettinger, D. C. Smith, D. F. McDermott, J. D. Powderly, R. D. Carvajal, J. A. Sosman, M. B. Atkins, P. D. Leming, D. R. Spigel, S. J. Antonia, L. Horn, C. G. Drake, D. M. Pardoll, L. Chen, W. H. Sharfman, R. A. Anders, J. M. Taube, T. L. McMiller, H. Xu, A. J. Korman, M. Jure-Kunkel, S. Agrawal, D. McDonald, G. D. Kollia, A. Gupta, J. M. Wigginton, M. Sznol, Safety, activity, and immune correlates of anti–PD-1 antibody in cancer. *N. Engl. J. Med.* **366**, 2443–2454 (2012). doi:10.1056/NEJMoa1200690 Medline

3. K. K. Frese, A. Neesse, N. Cook, T. E. Bapiro, M. P. Lolkema, D. I. Jodrell, D. A. Tuveson, *nab*-Paclitaxel potentiates gemcitabine activity by reducing cytidine deaminase levels in a mouse model of pancreatic cancer. *Cancer Discov.* **2**, 260–269 (2012). doi:10.1158/2159-8290.CD-11-0242 Medline

4. C. Feig, A. Gopinathan, A. Neesse, D. S. Chan, N. Cook, D. A. Tuveson, The pancreas cancer microenvironment. *Clin. Cancer Res.* **18**, 4266–4276 (2012). doi:10.1158/1078-0432.CCR-11-3114 Medline

5. R. Straussman, T. Morikawa, K. Shee, M. Barzily-Rokni, Z. R. Qian, J. Du, A. Davis, M. M. Mongare, J. Gould, D. T. Frederick, Z. A. Cooper, P. B. Chapman, D. B. Solit, A. Ribas, R. S. Lo, K. T. Flaherty, S. Ogino, J. A. Wargo, T. R. Golub, Tumour micro-environment elicits innate resistance to RAF inhibitors through HGF secretion. *Nature* **487**, 500–504 (2012). doi:10.1038/nature11183 Medline

6. T. R. Wilson, J. Fridlyand, Y. Yan, E. Penuel, L. Burton, E. Chan, J. Peng, E. Lin, Y. Wang, J. Sosman, A. Ribas, J. Li, J. Moffat, D. P. Sutherlin, H. Koeppen, M. Merchant, R. Neve, J. Settleman, Widespread potential for growth-factor-driven resistance to anticancer kinase inhibitors. *Nature* **487**, 505–509 (2012). doi:10.1038/nature11249 Medline

7. W. Plunkett, P. Huang, Y. Z. Xu, V. Heinemann, R. Grunewald, V. Gandhi, Gemcitabine: Metabolism, mechanisms of action, and self-potentiation. *Semin. Oncol.* **22**, 3–10 (1995). Medline

8. J. Vande Voorde, S. Sabuncuoğlu, S. Noppen, A. Hofer, F. Ranjbarian, S. Fieuws, J. Balzarini, S. Liekens, Nucleoside-catabolizing enzymes in mycoplasma-infected tumor cell cultures compromise the cytostatic activity of the anticancer drug gemcitabine. *J. Biol. Chem.* **289**, 13054–13065 (2014). doi:10.1074/jbc.M114.558924 Medline

9. P. Lehouritis, J. Cummins, M. Stanton, C. T. Murphy, F. O. McCarthy, G. Reid, C. Urbaniak, W. L. Byrne, M. Tangney, Local bacteria affect the efficacy of chemotherapeutic drugs. *Sci. Rep.* **5**, 14554 (2015). doi:10.1038/srep14554 Medline

10. M. Kanehisa, S. Goto, KEGG: Kyoto encyclopedia of genes and genomes. *Nucleic Acids Res.* **28**, 27–30 (2000). doi:10.1093/nar/28.1.27 Medline

11. J. E. Craig, Y. Zhang, M. P. Gallagher, Cloning of the *nupC* gene of *Escherichia coli* encoding a nucleoside transport system, and identification of an adjacent insertion element, IS 186. *Mol. Microbiol.* **11**, 1159–1168 (1994). doi:10.1111/j.1365-2958.1994.tb00392.x Medline

12. J. Stritzker, S. Weibel, P. J. Hill, T. A. Oelschlaeger, W. Goebel, A. A. Szalay, Tumor-specific colonization, tissue distribution, and gene induction by probiotic *Escherichia coli* Nissle 1917 in live mice. *Int. J. Med. Microbiol. IJMM* **297**, 151–162 (2007). doi:10.1016/j.ijmm.2007.01.008 Medline

13. O. Jonas, H. M. Landry, J. E. Fuller, J. T. Santini Jr., J. Baselga, R. I. Tepper, M. J. Cima, R. Langer, An implantable microdevice to perform high-throughput in vivo drug sensitivity testing in tumors. *Sci. Transl. Med.* **7**, 284ra57 (2015). doi:10.1126/scitranslmed.3010564 Medline

14. S. Yuan, D. B. Cohen, J. Ravel, Z. Abdo, L. J. Forney, Evaluation of methods for the extraction and purification of DNA from the human microbiome. *PLOS ONE* **7**, e33865 (2012). doi:10.1371/journal.pone.0033865 Medline

15. A. Lyubimova, S. Itzkovitz, J. P. Junker, Z. P. Fan, X. Wu, A. van Oudenaarden, Single-molecule mRNA detection and counting in mammalian tissue. *Nat. Protoc.* **8**, 1743–1758 (2013). doi:10.1038/nprot.2013.109 Medline

16. E. Nistal, A. Caminero, A. R. Herrán, L. Arias, S. Vivas, J. M. R. de Morales, S. Calleja, L. E. S. de Miera, P. Arroyo, J. Casqueiro, Differences of small intestinal bacteria populations in adults and children with/without celiac disease: Effect of age, gluten diet, and disease. *Inflamm. Bowel Dis.* **18**, 649–656 (2012). doi:10.1002/ibd.21830 Medline

17. G. Ou, M. Hedberg, P. Hörstedt, V. Baranov, G. Forsberg, M. Drobni, O. Sandström, S. N. Wai, I. Johansson, M.-L. Hammarström, O. Hernell, S. Hammarström, Proximal small intestinal microbiota and identification of rod-shaped bacteria associated with childhood celiac disease. *Am. J. Gastroenterol.* **104**, 3058–3067 (2009). doi:10.1038/ajg.2009.524 Medline

18. A. Sivan, L. Corrales, N. Hubert, J. B. Williams, K. Aquino-Michaels, Z. M. Earley, F. W. Benyamin, Y. M. Lei, B. Jabri, M.-L. Alegre, E. B. Chang, T. F. Gajewski, Commensal *Bifidobacterium* promotes antitumor immunity and facilitates anti–PD-L1 efficacy. *Science* **350**, 1084–1089 (2015). doi:10.1126/science.aac4255 Medline

19. M. Vétizou, J. M. Pitt, R. Daillère, P. Lepage, N. Waldschmitt, C. Flament, S. Rusakiewicz, B. Routy, M. P. Roberti, C. P. M. Duong, V. Poirier-Colame, A. Roux, S. Becharef, S. Formenti, E. Golden, S. Cording, G. Eberl, A. Schlitzer, F. Ginhoux, S. Mani, T. Yamazaki, N. Jacquelot, D. P. Enot, M. Bérard, J. Nigou, P. Opolon, A. Eggermont, P.-L. Woerther, E. Chachaty, N. Chaput, C. Robert, C. Mateus, G. Kroemer, D. Raoult, I. G. Boneca, F. Carbonnel, M. Chamaillard, L. Zitvogel, Anticancer immunotherapy by CTLA-4 blockade relies on the gut

microbiota. *Science* **350**, 1079–1084 (2015). doi:10.1126/science.aad1329 Medline

20. B. D. Wallace, H. Wang, K. T. Lane, J. E. Scott, J. Orans, J. S. Koo, M. Venkatesh, C. Jobin, L.-A. Yeh, S. Mani, M. R. Redinbo, Alleviating cancer drug toxicity by inhibiting a bacterial enzyme. *Science* **330**, 831–835 (2010). doi:10.1126/science.1191175 Medline

21. J. Cummins, M. Tangney, Bacteria and tumours: Causative agents or opportunistic inhabitants? *Infect. Agent. Cancer* **8**, 11 (2013). doi:10.1186/1750-9378-8-11 Medline

22. T. Yu, F. Guo, Y. Yu, T. Sun, D. Ma, J. Han, Y. Qian, I. Kryczek, D. Sun, N. Nagarsheth, Y. Chen, H. Chen, J. Hong, W. Zou, J.-Y. Fang, *Fusobacterium nucleatum* promotes chemoresistance to colorectal cancer by modulating autophagy. *Cell* **170**, 548–563.e16 (2017). doi:10.1016/j.cell.2017.07.008 Medline

23. T. Danino, A. Prindle, G. A. Kwong, M. Skalak, H. Li, K. Allen, J. Hasty, S. N. Bhatia, Programmable probiotics for detection of cancer in urine. *Sci. Transl. Med.* **7**, 289ra84 (2015). doi:10.1126/scitranslmed.aaa3519 Medline

24. J. G. Caporaso, C. L. Lauber, W. A. Walters, D. Berg-Lyons, J. Huntley, N. Fierer, S. M. Owens, J. Betley, L. Fraser, M. Bauer, N. Gormley, J. A. Gilbert, G. Smith, R. Knight, Ultra-high-throughput microbial community analysis on the Illumina HiSeq and MiSeq platforms. *ISME J.* **6**, 1621–1624 (2012). doi:10.1038/ismej.2012.8 Medline

25. J. G. Caporaso, J. Kuczynski, J. Stombaugh, K. Bittinger, F. D. Bushman, E. K. Costello, N. Fierer, A. G. Peña, J. K. Goodrich, J. I. Gordon, G. A. Huttley, S. T. Kelley, D. Knights, J. E. Koenig, R. E. Ley, C. A. Lozupone, D. McDonald, B. D. Muegge, M. Pirrung, J. Reeder, J. R. Sevinsky, P. J. Turnbaugh, W. A. Walters, J. Widmann, T. Yatsunenko, J. Zaneveld, R. Knight, QIIME allows analysis of high-throughput community sequencing data. *Nat. Methods* **7**, 335–336 (2010). doi:10.1038/nmeth.f.303 Medline

26. D. McDonald, M. N. Price, J. Goodrich, E. P. Nawrocki, T. Z. DeSantis, A. Probst, G. L. Andersen, R. Knight, P. Hugenholtz, An improved Greengenes taxonomy with explicit ranks for ecological and evolutionary analyses of bacteria and archaea. *ISME J.* **6**, 610–618 (2012). doi:10.1038/ismej.2011.139 Medline

27. D. Knights, J. Kuczynski, O. Koren, R. E. Ley, D. Field, R. Knight, T. Z. DeSantis, S. T. Kelley, Supervised classification of microbiota mitigates mislabeling errors. *ISME J.* **5**, 570–573 (2011). doi:10.1038/ismej.2010.148 Medline

28. D. Knights, J. Kuczynski, E. S. Charlson, J. Zaneveld, M. C. Mozer, R. G. Collman, F. D. Bushman, R. Knight, S. T. Kelley, Bayesian community-wide culture-independent microbial source tracking. *Nat. Methods* **8**, 761–763 (2011). doi:10.1038/nmeth.1650 Medline